ELSEVIER

Journal of Organometallic Chemistry 558 (1998) 147–153

Journal of Organometallic Chemistry

The synthesis, solid state conductivity and X-ray crystal structure of $[Fe\{\eta^5\text{-}C_5H_5)(E\text{-}\eta^5\text{-}C_5H_4{-}CH{=}CH\text{-}9\text{-}C_{16}H_9)][1,4\text{-}\{(CN)_2C{=}\}_2C_6H_4]$

James D. McKinney [a], Paul A. Anderson [a], Thomas A. Hamor [a], Christopher J. Jones [a,*], Keith Paxton [a], Adrian Porch [b]

[a] *School of Chemistry, University of Birmingham, Edgbaston, Birmingham, B15 2TT, UK*
[b] *School of Electronic and Electrical Engineering, University of Birmingham, Edgbaston, Birmingham, B15 2TT, UK*

Received 1 November 1997; received in revised form 18 December 1997

Abstract

The new compounds $[Fe(\eta^5\text{-}C_5H_5)(E\text{-}\eta^5\text{-}C_5H_4{-}CH{=}CH\text{-}9\text{-}C_{16}H_9)]$, $[Fe(\eta^5\text{-}C_5H_5)(E\text{-}\eta^5\text{-}C_5H_4{-}CH{=}CH\text{-}9\text{-}C_{16}H_9)][(CN)_2C{=}C(CN)_2]$ and $[Fe(\eta^5\text{-}C_5H_5)(E\text{-}\eta^5C_5H_4{-}CH{=}CH\text{-}9\text{-}C_{16}H_9)][1,4\text{-}\{(CN)_2C{=}\}_2C_6H_4]$ have been synthesized and characterized by their mass, IR and ^1H NMR spectra. The crystal structure of the latter compound contains 1,2-ferrocenyl-pyrenyl-ethene and $1,4\text{-}\{(CN)_2C{=}\}_2C_6H_4$ (TCNQ) molecules alternating in stacks characteristic of π–π^* electron donor–acceptor complexes. The pyrene and TCNQ moieties are nearly parallel, angle of tilt 5.3°, with interplanar separations of 3.33 and 3.42 Å. Microwave cavity perturbation measurements have been used to show that this solid behaves as a normal semi-conductor below 176 K.

Keywords: Ferrocenyl; Semiconductor; Crystal structure; Solid state conductivity; EPR

---

1. Introduction

The ferrocenyl moiety is a robust organometallic electron donor group which has been used in the preparation of new molecular materials exhibiting non-linear optical (NLO) [1–5] and ferromagnetic properties [6–8]. Two reasons for selecting the ferrocenyl group for such studies are its good electron donor properties and its well established substitution chemistry, which allows access to a wide variety of derivatives designed to serve particular functions. This has been particularly important in the design and synthesis of new molecular materials with second order NLO properties [1–5]. An important feature of such molecular materials is the packing arrangement adopted by molecules in the solid state, as this can have a major influence on the bulk properties of the molecular material. One parameter which may be exploited when attempting to obtain favourable packing arrangements is molecular shape [4,5]. In this work we describe the construction of an L-shaped molecule in which a ferrocenyl donor group is linked to a planar polyaromatic moiety. The addition of a planar acceptor molecule of suitable size to this L-shaped donor might then complete a parallelepiped which could pack readily into an ordered stacked lattice (Fig. 1). Geometrically the ferrocenyl group is suitable for this purpose since its 'height', the spacing between the cyclopentadienyl rings, is ca. 3.3 Å, similar to the interplanar spacing in π–π^* donor–acceptor complexes. The planar electron acceptor molecules tetracyanoethene (TCNE) and tetracyanoquinone dimethide (TCNQ) can form charge transfer salts with polyaromatic electron donors and were selected as suitable acceptors to occupy the vacant area within the L-shape and form a regularly shaped donor–acceptor unit. In order to assess the success of this strategy the solid state structure of the compound produced from TCNQ and *trans*-1-ferrocenyl-2-pyrenyl ethene has been deter-

---

* Corresponding author.

0022-328X/98/$19.00 © 1998 Elsevier Science S.A. All rights reserved.
PII S0022-328X(98)00392-1

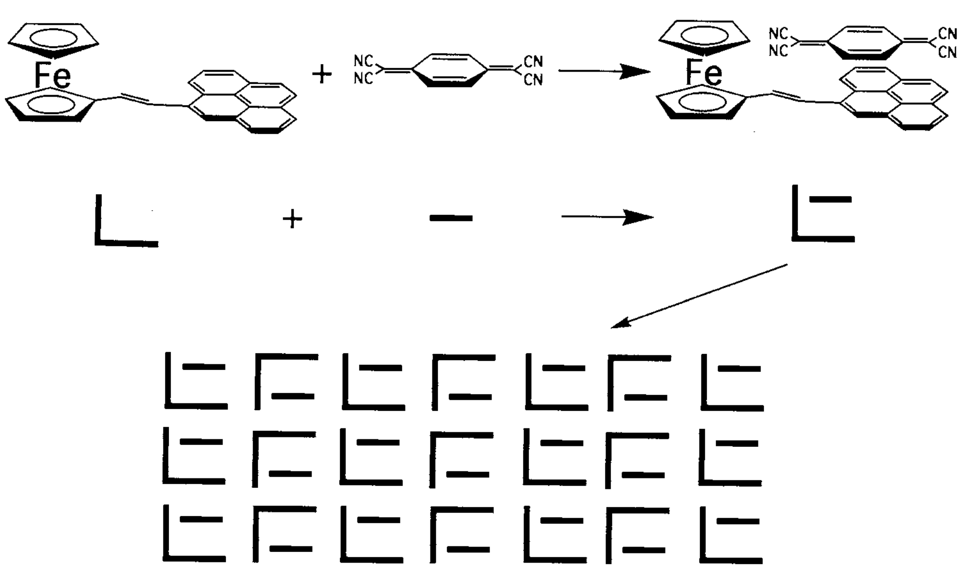

Fig. 1. A schematic representation of the formation of a stacked structure involving an L-shaped donor molecule and a planar acceptor molecule.

mined. Microwave cavity perturbation measurements provide a convenient means of investigating the solid state electrical conductivity of powdered solids [9,10]. Previously this method has been successfully applied to the study of non-molecular materials. In this paper we describe its application to measuring the solid state conductivity of the molecular material formed from TCNQ and *trans*-1-ferrocenyl-2-pyrenyl ethene.

2. Results and discussion

2.1. Synthetic studies

1,2-Ferrocenyl-pyrenyl-ethene (**1**, [Fe(η^5-C_5H_5)(E-η^5-C_5H_4–CH=CH-9-$C_{16}H_9$)]) was synthesized from [Fe(η^5-C_5H_5)(E-η^5-C_5H_4–CH_2PPh_3)] and pyrene-9-carboxyaldehyde using a modification of the procedure described for the preparation of [Fe(η^5-C_5H_5)(E-η^5-C_5H_4–CH=CH-4-$C_6H_4NO_2$)] [3]. This compound was then reacted with TCNE or TCNQ to form the respective compounds [Fe(η^5-C_5H_5)(E-$\eta^5$$C_5H_4$–CH=CH-9-$C_{16}H_9$)][$(CN)_2C$=$C(CN)_2$], **2**, and [Fe($\eta^5$-$C_5H_5$)($E$-$\eta^5$-$C_5H_4$–CH=CH-9-$C_{16}H_9$)][1,4-{$(CN)_2C$=}$_2C_6H_4$], **3**. The formulation of these materials was confirmed by IR and ^{1}H NMR spectroscopy, by elemental analyses and by mass spectrometry. The EI mass spectrum of **1** contained a molecular ion at m/z 412 in accord with its formulation as [Fe(η^5-C_5H_5)(E-$\eta^5$$C_5H_4$–CH=CH-9-$C_{16}H_9$)]. In the cases of **2** and **3** both positive and negative ion fast atom bombardment (FAB) mass spectra were recorded. In each case an ion due to the ferrocenyl pyrene cation was observed at m/z 412 in the positive ion FAB mass spectra. The negative ion FAB mass spectra contained ions at m/z 128 in the case of **2** and 204 in the case of **3** confirming the presence of the respective TCNE and TCNQ components of the compounds. The infra-red spectra of **2** and **3** contained bands consistent with the presence of the ferrocenyl-pyrenyl-ethene donor in addition to bands due to the TCNE or TCNQ components at ca. 2200 cm^{-1}, assigned to $\nu_{C\equiv N}$, and at ca. 820 cm^{-1}, assigned to the C≡N bending mode.

The ^{1}H NMR spectrum of **1** contained the expected signals arising from the ferrocenyl group. The unsubstituted C_5H_5 ring gives rise to a singlet at essentially the same shift as that found for ferrocene itself. The monosubstituted C_5H_4 ring gives rise to an unsymmetrical pair of unresolved triplets corresponding to an A_2B_2 spectrum with J(adjacent) = J(cross) and small compared to the chemical shift difference between $H_{2,5}$ and $H_{3,4}$ [11]. These signals appear downfield of the C_5H_5 singlet, showing that all four ring protons are deshielded by the aryl rings of the pyrene substituent. Signals associated with pyrenyl protons were also present having a total relative area of nine with respect to the ferrocenyl protons. The ethenyl protons in **1** exhibit a vicinal coupling of 16 Hz consistent with the expected *trans*-stereochemistry. The ^{1}H NMR spectrum of **2** is almost identical to that of **1** showing that there is little interaction between the acceptor and the donor in solution. Similarly, the ^{1}H NMR spectrum of **3** differs very little from that of **1** except for the appearance of a singlet at 7.35 ppm corresponding to the four equivalent protons on the aromatic ring of the TCNQ component. In accord with this observation the solution conductivities of 10^{-4} mol dm^{-3} solutions of **2** and **3** in acetonitrile were respectively 12 and 13 Ω^{-1} cm^2 mol^{-1} showing that the solutions are essentially

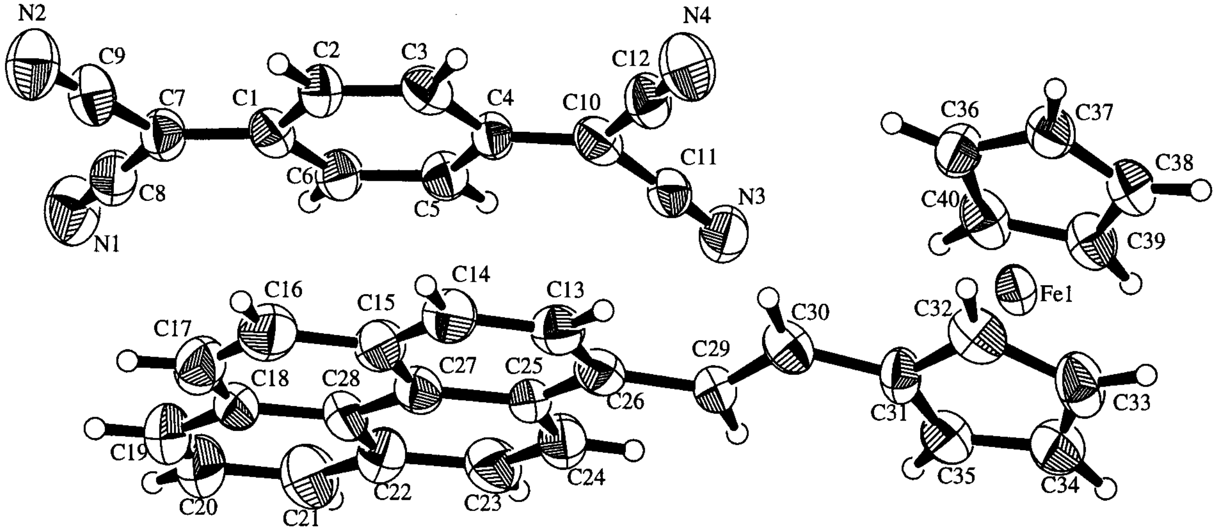

Fig. 2. The X-ray crystal structure of $[Fe(\eta^5\text{-}C_5H_5)(E\text{-}\eta^5\text{-}C_5H_4\text{–}CH{=}CH\text{-}9\text{-}C_{16}H_9)][1,4\text{-}\{(CN)_2C{=}\}_2C_6H_4]$ **3**.

non-conducting and that electron transfer does not occur in solution to any significant extent. Solid samples of **2** and **3** were found to be diamagnetic over the temperature range 6–300 K[1].

2.2. Electrochemical studies

The electrochemical properties of **1** and **3** were investigated by cyclic voltammetry. Both compounds showed a reversible oxidation wave associated with the ferrocenyl moiety with ΔE_p values similar to that of the ferrocene standard indicating that the oxidation is reversible. Compared to the ferrocene standard the oxidation potentials of the ferrocenyl groups in **1** and **3** are shifted to more negative potentials by 150 mV. This is in accord with the pyrene group acting as an electron donor towards the ferrocenyl group in **1** or **3**, stabilizing the oxidized form with respect to ferrocene itself. In the case of **3** a reduction wave is also observed at -0.80 V which may be attributed to the reduction of the TCNQ molecule. The ferrocenyl group in turn should similarly act as an electron donor substituent towards the pyrenyl group enhancing its capacity to interact with acceptor molecules.

2.3. Structural studies

In order to assess the success, or otherwise, of the strategy to produce a stacked molecular packing arrangement, illustrated in Fig. 1, a single crystal X-ray diffraction study of **3** was carried out to determine the room temperature solid state structure. Crystals were grown in air from a solution of the compound in dichloromethane over which a layer of hexane was present. The pyrene donor and TCNQ acceptor structures are shown in Fig. 2 [12] and the packing arrangement in Fig. 3 [13]. The crystal structure comprises $[Fe\{\eta^5\text{-}C_5H_5)(E\text{-}\eta^5C_5H_4\text{–}CH{=}CH\text{-}9\text{-}C_{16}H_9)]$ and TCNQ molecules alternating in plane-to-plane stacks characteristic of π–π^* electron donor acceptor complexes [14,15], and also a water molecule presumed to arise adventitiously from the air in contact with the crystallization solvents. This latter molecule forms a hydrogen-bonded dimer with a symmetry-related water molecule but is not involved in any other interactions.

The pyrene and TCNQ moieties are both roughly planar (to within 0.06 and 0.18 Å respectively) and stack nearly parallel to one another with only a slight inclination of ca. 5.3(1)°. The cyclopentadienyl rings of the ferrocene are inclined at 16.9° to the pyrene least squares plane. A more accurate description of the pyrene residue is that it is bent by 3.3(2)° about the C(18)–C(28)–C(27)–C(25) line, with the two fused naphthalene moieties each planar to within 0.03 Å, similar to the structure of pyrene itself [16–20]. The TCNQ molecule has a planar six-membered ring, the two $C(CN)_2$ sustituents being displaced by 0.04–0.36 Å on the same side of the ring plane. In contrast, TCNQ itself has a planar structure [21,22]. The interplanar spacings are approximately 3.33 Å [pyrene-TCNQ (x, y, z)] and 3.42 Å [pyrene-TCNQ $(x, y, -1+z)$]. These values may be compared with the pyrene-TCNQ interplanar separation of 3.50 Å and dihedral angle of 6.3° in the 1:1 molecular complex of pyrene and TCNQ [14]. Projections of the TCNQ molecules at (x, y, z) and $(x, y, -1+z)$ onto the mean plane of the pyrene residue are shown in Fig. 4 [12]. The degree of offset is similar, but not identical, to that found in the crystal structure of the pyrene-TCNQ complex [14].

---

[1] made using a SQUID magnetometer in the School of Physics and Space Science, The University of Birmingham.

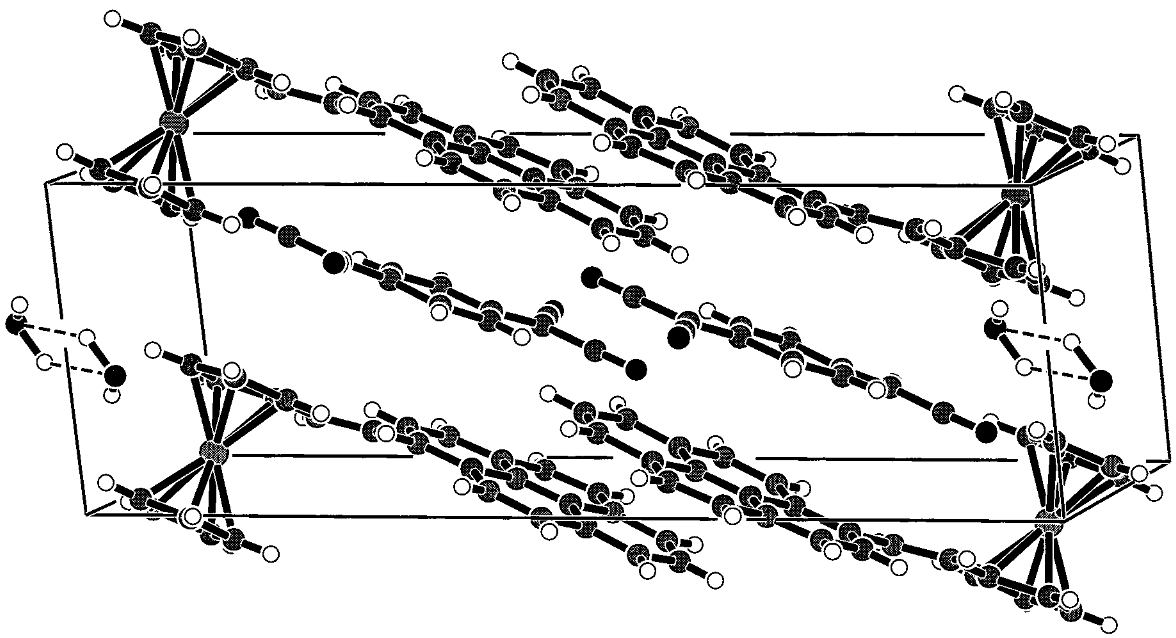

Fig. 3. The packing arrangement of [Fe(η^5-C_5H_5)(E-η^5-C_5H_4–CH=CH-9-$C_{16}H_9$)][1,4-{$(CN)_2C$=}$_2C_6H_4$], **3** x-axis towards the viewer, y down the page, z across the page.

The closest distances between the centres, Fe(ferrocene) and N(TCNQ), are 4.53(1) and 4.77(1) Å which are over 1 Å shorter than those found in Miller's ferromagnetic molecular salts [6–8,23]. In the chain direction the intrachain Fe···Fe separation is approximately 9.3 Å and comparable to the distances found in Miller's [6–8,23] and Mingos' [24] charge transfer salts. The structure shows that the combination of the planar pyrene substituent, which is capable of acting as an electron donor in its own right, with the ferrocenyl electron donor group produces an anisotropic molecule which, when packed in a lattice, can accommodate a planar electron acceptor molecule in the cavities produced. This leads to closer contacts than in previous examples of DA compounds of this type.

2.4. Solid state conductivity measurements

Solid state electrical conductivity measurements were carried out on a powdered sample of **3** using microwave cavity perturbation measurements. This method, originally applied to the investigation of anisotropy in the conducting properties of cuprate superconductors [9], has been developed in recent years in response to problems often associated with the measurement of electrical conductivity in new materials [8,9,25,26]. The technique involves the measurement of the change in resonant frequency and resonant bandwidth which occurs on introduction of a known volume of the sample into a quarterwave copper hairpin cavity resonating at around 3 GHz. At this high frequency the effects of powder intergrain contacts are negligible and the method therefore has the advantage of probing directly the intragrain cobnductivity. Provided that the microwaves penetrate fully the sample, the change in resonant bandwidth is proportional to the sample conductivity. It can be shown that this condition is violated only by samples exhibiting very high values of conductivity, many orders of magnitude higher than those reported here for **3**. Values for the conductivity and relative permittivity of the sample can be extracted from the resonant frequency and bandwidth data through appropriate modelling. Approximations in the process result in a systematic error of around ± 30% in the absolute values of the measured conductivities. For a given sample, however, this error is fixed and much smaller changes in the conductivity occuring, for example, as a function of temperature (see below) are reliably detected. By dispensing with the need for sample contacts, the measurements provide a quick and convenient means of evaluating the conductivity of interesting new compounds whose materials properties may not yet be optimized. The technique is sufficiently versatile to handle a wide range of 'difficult' samples and is particularly useful for samples in the form of microcrystalline powders, those which are not easily sintered, and those which are air- or moisture-sensitive. With the added possibility of detecting anisotropy in the conducting properties [10], we believe that it is well suited to providing information about the electrical conductivity of molecular solids and, to our knowledge, this represents the first example of its application to such materials.

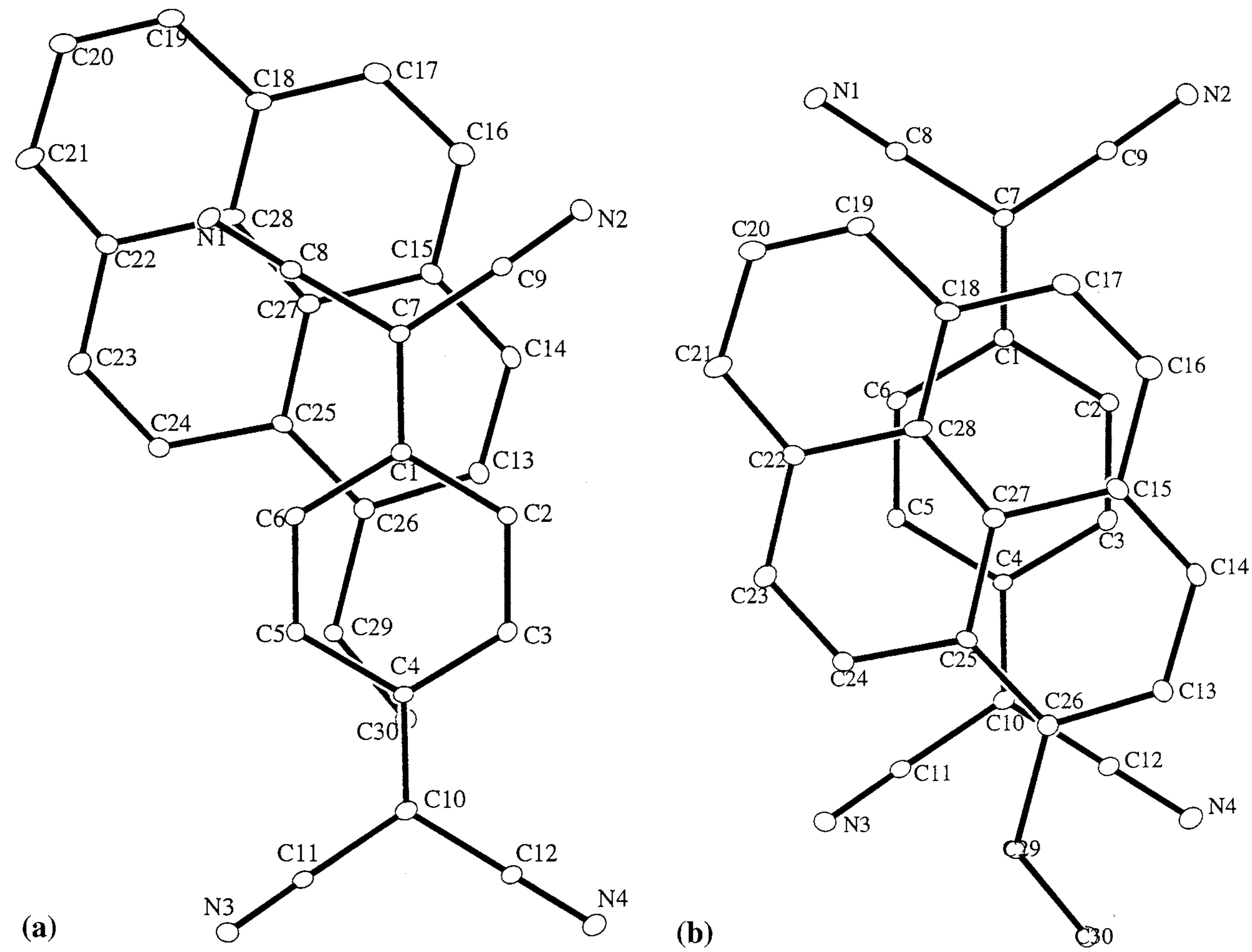

Fig. 4. Projections of the TCNQ molecules at (a), (x, y, z) and (b), $(x, y, -1+z)$ onto the mean plane of the pyrene residue.

The relationship between temperature and the electrical conductivity of **3** is shown in Fig. 5. Between the temperatures 6 and 176 K **3** behaves broadly as a typical semi-conductor showing increasing conductivity with increasing temperature. At 176 K the electrical conductivity of **3** is 2.8×10^{-4} S cm^{-1} and this would normally have been expected to rise to ca. 9×10^{-4} S cm^{-1} at room temperature. However, above 176 K there is, in fact, a dramatic decrease in conductivity with increasing temperature. This type of temperature dependence is normally associated with metallic conduction and could arise from electronic effects resulting from the increased population of higher energy levels at the higher temperature. However, the maximum value of conductivity measured is relatively modest and the observed change in behaviour at 176 K could simply arise from a phase transition in **3** changing the properties of the bulk material. Attempts to investigate the solid state structure of the crystalline compound at low temperatures were unsuccessful as the crystals decrepitated and no definitive evidence for such a phase change could be obtained.

2.5. Conclusion

The structural results obtained here validate the strategy of using molecular shape in an attempt to obtain a favourable stacked packing arrangement in a two component molecular donor–acceptor system. In the example studied this leads to a diamagnetic molecular material which behaves as a semiconductor at low temperature. The work also demonstrates the utility of microwave cavity perturbation measurements as a convenient method for screening molecular materials for solid state electrical conductivity properties.

3. Experimental

3.1. Synthetic studies

Reaction solvents were purified by distillation under nitrogen from standard drying agents before use. The reagent $FcCH_2PPh_3$ was prepared by the literature method [27]. All commercial chemicals were pre-dried before use but otherwise were used as received unless otherwise stated. All column chromatography was carried out on silica gel and alumina from Merck (70–230 mesh) with the eluants stated.

3.2. Physical measurements

IR spectra were recorded from KBr discs using a Perkin Elmer 1600 series FT–IR spectrophotometer. ^{1}H NMR 300 MHz spectra were recorded using a Brucker AC300 spectrometer. Mass spectra were recorded using a Kratos MS 80 instrument with positive or negative ion fast atom bombardment of a NOBA matrix. Cyclic voltammetry was carried out using an EG&G model 174A polarographic analyser, with ca. 10^{-3} mol dm^{-3} solutions under dry N_2 in dry dichloromethane. A Pt bead working electrode was used, with 0.2 mol dm^{-3} [Bu^n_4N][BF_4] as supporting electrolyte, and a scan rate of 200 mV s^{-1}. Potentials are quoted relative to ferrocene (ΔE_p 70 mV) added as an internal standard. Solution conductivity measurements were recorded using a PTI 58 digital conductivity meter. Solid state conductivity measurements were made according to the microwave cavity perturbation method described elsewhere [10,28].

Elemental analyses were performed by the Microanalytical Laboratory of the University of Sheffield.

3.3. [Fe(η^5-C_5H_5)(E-η^5-C_5H_4–CH=CH-9-$C_{16}H_9$)], ***1***

The procedure described in the literature [3] to prepare *E*-[Fe(η^5-C_5H_5)(*E*-η^5-C_5H_4–CH=CHNO$_2$-4)] was followed using [Fe(η^5-C_5H_5)(*E*-η^5-C_5H_4–CH_2PPh_3)] (2.08 g, 4.52 mmol) and pyrene-9-carboxyaldehyde (1.70 g, 7.38 mmol). Further purification of **1** was achieved by alumina column chromatography using petroleum ether (40–60°)/ethyl acetate (95:5) as the eluants. An orange gelatinous solid was formed which was further purified by recrystallization from *n*-heptane to yield an orange crystalline solid (1.61 g, 53%). (Found: C, 81.6; H, 4.46; N, 0.00. $C_{28}H_{20}Fe$, requires, C, 81.6; H, 4.89; N, 0.00%): ^{1}H ($CDCl_3$) δ; 8.10 (9H, m, $C_{16}H_9$), 7.10 (1H, d, 16.2 Hz, CH=C*H*), 7.03 (1H, d, 16.2 Hz, C*H*=CH), 4.84, 4.48 (2H, br, 2H, br, η^5-C_5H_4), 4.35 (5H, s, η^5-C_5H_5): Mass Spectrum *m*/*z* (*I*%); EI, 412 (100) [M]$^+$, 347 (26) [M-C_5H_5]$^+$, 289 (14) [M-C_5H_5Fe]$^+$; E_f, -0.15 V, ΔE_p 65 mV.

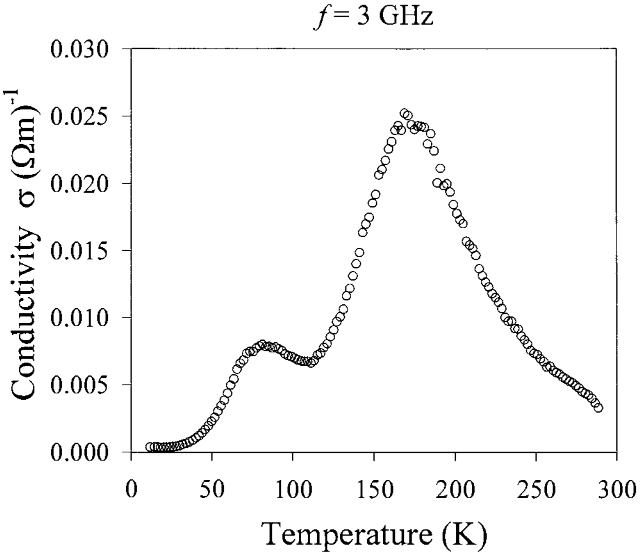

Fig. 5. A graph to show the relationship between temperature (K) and solid state conductivity (Ωm)$^{-1}$ in [Fe(η^5-C_5H_5)(*E*-η^5-C_5H_4–CH=CH-9-$C_{16}H_9$)][1,4-{$(CN)_2C$=}$_2C_6H_4$] **3**.

3.4. [Fe(η^5-C_5H_5)(E-η^5-C_5H_4–CH=CH-9-$C_{16}H_9$)]-[TCNE], ***2***

A hot solution of TCNE (0.09 g, 0.7 mmol) in acetonitrile (20 cm^3) was added dropwise, under an inert atmosphere, to a solution of **1** (0.25 g, 0.6 mmol) in acetonitrile (20 cm^3) under reflux. The mixture was refluxed for a further 10 min then allowed to cool slowly over a 4 h period. A brown precipitate formed and was collected by filtration and washed with copious amounts of first toluene then *n*-hexane. Further purification was achieved by recrystallizing the material twice from dichloromethane/hexane to yield a purple solid (0.18 g, 55%). (Found: C, 75.4; H, 3.63; N, 10.2. $C_{34}H_{20}N_4Fe$, requires, C, 75.6; H, 3.73; N, 10.4%): ν_{max} (CN) 2203m cm^{-1}: ^{1}H ($CDCl_3$) δ; 8.05 (9H, m, $C_{16}H_9$), 7.15 (1H, d, $J = 16.2$ Hz, C*H*-=CH), 7.05 (1H, d, $J = 16.2$ Hz, CH=C*H*-), 4.84, 4.48 (2H, t, 2H, t, $J = 1.7$ Hz, η^5-C_5H_4), 4.35 (5H, s, η^5-C_5H_5): Mass Spectrum *m*/*z* (*I*%); +ve FAB, 412 (100) [M$^+$], 347 (26) [M$^+$-C_5H_5], 289 (14) [M$^+$-C_5H_5Fe]; −ve FAB, 128 (100) [M$^-$]; Λ_m, 12 Ω cm^2 mol^{-1}.

3.5. [Fe(η^5-C_5H_5)(E-η^5-C_5H_4–CH=CH-9-$C_{16}H_9$)]-[TCNQ], ***3***

The preceding procedure was followed using TCNQ (0.14 g, 0.7 mmol) and *E*-Fc–CH=CH-9-Pyrene (0.25 g, 0.6 mmol) in acetonitrile (20 cm^3). The washed precipitate obtained was further purified by recrystallization from dichloromethane/hexane to yield purple crystals (0.28 g, 75%). (Found: C, 77.7; H, 3.71; N, 9.17. $C_{40}H_{24}N_4Fe$, requires, C, 77.9; H, 3.92; N, 9.09%): ν_{max} (CN) 2216m cm^{-1}: ^{1}H ($CDCl_3$) δ; 8.05 (9H, m, $C_{16}H_9$), 7.35 (4H, s, TCNQ), 7.13 (1H, d, $J = 16.2$ Hz, C*H*-=CH), 7.05 (1H, d, $J = 16.2$ Hz, CH=C*H*), 4.84, 4.48 (2H, t, 2H, t, $J = 1.7$ Hz, η^5-C_5H_4), 4.35 (5H, s, η^5-C_5H_5): Mass Spectrum *m*/*z* (*I*%); +ve FAB, 412 (100)

$[M^+]$, 347 (26) $[M^+\text{-}C_5H_5]$, 289 (14) $[M^+\text{-}C_5H_5Fe]$; −ve FAB, 204 (100) $[M^-]$, 166 (30) $[M^-\text{-}CNC]$ 153 (36); Λ_m, 13 Ω cm^2 mol^{-1}; λ_{max} nm (ϵ dm^3 mol^{-1} cm^{-1}) 233 (62800), 281 (3770), 297sh (28500), 380sh (154000), 395 (190000), 460 (6410); E_f, −0.15 V, ΔE_p 64 mV and E_f, −0.80 V, ΔE_p 74 mV.

3.6. Structural studies

$C_{28}H_{20}Fe.C_{12}H_4N_4.H_2O$, $M_r = 634.5$, triclinic, space group P-1 $a = 9.297(4)$, $b = 21.991(7)$, $c = 7.799(5)$ Å, $\alpha = 93.11(3)$, $\beta = 101.74(3)$, $\gamma = 82.80(3)°$, $V = 1548(1)$ Å^3, $Z = 2$, $D_c = 1.361$ g cm^{-3}, $F(000) = 656$, μ(Mo-K$_\alpha$) $= 0.527$ mm^{-1}, $\lambda = 0.71073$ Å.

Data were collected from a weakly diffracting crystal of size 0.3 × 0.2 × 0.2 mm mounted on a Rigaku *R*-Axis II area-detector diffractometer using graphite monochromated MoK$_\alpha$ radiation. Thirty-six 5° oscillation exposures were made with crystal to detector distances 80 mm. A total of 4640 reflections, in the range $0.9 < \theta < 25.2°$, having $I > \sigma(I)$, were measured. Of these 3152 were independent (R_{int} 0.0475) and were used in the analysis. The structure was determined [28] by direct methods and refined [29] on F^2 by least squares using anisotropic displacement parameters for the non-hydrogen atoms. The hydrogen atoms of the complex were placed in calculated positions 'riding' on their respective bonded atoms. Those of the water molecule were located from a difference map, but their parameters were not refined. Refinement was terminated when all shift/e. s.d. ratios were < 0.01 and R, wR_2 were 0.0991, 0.2724, respectively with $w = 1/[\sigma^2(F_o^2) + (0.178P)^2 + 0.27P]$ where $P = (F_o^2 + 2F_c^2)/3$ The residual electron density was within the range ± 0.64 eÅ^{-3}. For 2612 reflections having $I > 2\sigma(I)$, $R = 0.0877$[2]. The high R values are surprising in view of the satisfactorily low values of R_{int} and residual electron density, and may be attributed to the poor quality of the available crystals.

Acknowledgements

We are grateful to M. Slaski for magnetic measurements and to the EPSRC for support through a studentship (J.D.McK.) and grant GR/G44390. We also thank the EPSRC and the University of Birmingham for funds to purchase the *R*-Axis II diffractometer.

References

[1] M.L.H. Green, S.R. Marder, M.E. Thompson, J.A. Bandy, D. Bloor, P.V. Kolinsky, R.J. Jones, Nature (London) 330 (1987) 360.

[2] S.R. Marder, J.W. Perry, W.P. Schaefer, Science 245 (1989) 626.

[3] H.E. Bunting, M.L.H. Green, S.R. Marder, M.E. Thompson, D. Bloor, P.V. Kolinsky, R.J. Jones, Polyhedron 11 (1992) 1489.

[4] B.J. Coe, J.-D. Foulon, T.A. Hamor, C.J. Jones, J.A. McCleverty, D. Bloor, G.H. Cross, T.L. Axon, J. Chem. Soc. Dalton Trans. (1994) 3427.

[5] B.J. Coe, J.-D. Foulon, T.A. Hamor, C.J. Jones, J.A. McCleverty, D. Bloor, G.H. Cross, T.L. Axon, J. Chem. Soc. Dalton Trans. (1995) 673.

[6] G.A. Candela, L.J. Swartzzendruber, J.S. Miller, M.J. Rice, J. Am. Chem. Soc. 101 (1979) 2755.

[7] J.S. Miller, A.J. Epstein, W.M. Reiff, Chem. Rev. 88 (1988) 201.

[8] J.S. Miller, A.J. Epstein, W.M. Reiff, Acc. Chem. Res. 40 (1988) 240.

[9] J.R. Waldram, A. Porch, H.M. Cheah, Physica C 332 (1994) 189.

[10] P.A. Anderson, A.R. Armstrong, A. Porch, P.P. Edwards and L.J. Woodall, J. Phys. Chem. 101 (1998) 9892.

[11] Rosenblum, Chemistry of the Iron Group Metallocenes, Wiley, New York, pp. 44 and 215, 1965.

[12] C.K. Johnson, ORTEP. Report ORNL-5138, Oak Ridge National Laboratory, Oak Ridge, TN, USA, 1976.

[13] J.W. Lauher, CHARON. Graphics Program for Postscript Printers, Research Foundation of the State University of New York, 1989.

[14] C.K. Prout, I.J. Tickle, J.D. Wright, J. Chem. Soc. Perk. Trans. II (1973) 528.

[15] J.C. Barnes, W. Golnazarians, Acta Cryst. C43 (1987) 549.

[16] A.C. Hazell, F.K. Larsen, M.S. Lehmann, Acta Crystallogr. B28 (1972) 2977.

[17] R. Allmann, Z. Krystallogr. 132 (1970) 129.

[18] A. Camerman, J. Trotter, Acta Crystallogr. 18 (1965) 636.

[19] Y. Kai, F. Hamu, N. Yasuoka, N. Kasui, Acta Crystallogr. B34 (1978) 1263.

[20] A.I. Pertsin, Yu.P. Ivanov, A.I. Kitaigorodskii, Kristallografiya 26 (1981) 115.

[21] M. Yingde, Z. Jintao, Z. Zhigui, Y. Ke, Z. Hengbin, G. Chunxiao, W. Zongu, Y. Ling, J. Songchun, F. Yuguo, Jilin Daxue Ziran Kex. Xue. (1988) 99.

[22] R.E. Long, R.A. Sparks, K.N. Trueblood, Acta Crystallogr. 18 (1965) 932.

[23] J.S. Miller, J.C. Calabrese, H. Römmelmann, S.R. Chittipeddi, J.H. Zhang, W.M. Reiff, A.J. Epstein, J. Am. Chem. Soc. 109 (1987) 769.

[24] Y.-K. Yan, D.M.P. Mingos, Chem. Soc. Rev. 24 (1995) 203.

[25] P.A. Anderson, L.J. Woodall, A. Porch, A.R. Armstrong, I. Hussain, P.P. Edwards, Mater. Res. Soc. Symp. Proc. 384 (1995) 9.

[26] P.P. Edwards, P.A. Anderson, L.J. Woodall, A. Porch, A.R. Armstrong, Mater. Sci. Eng. A 217/218 (1996) 198.

[27] P.L. Pauson, W.E. Watts, J. Chem. Soc. (1963) 2990.

[28] Molecular Structure Corporation, TeXsan. Single Crystal Structure Analysis Software, version 1.6. MSC, 3200 Research, Forest Drive, TX 77381, USA, 1993.

[29] G.M. Sheldrick, SHELXL-93. Program for Crystal Structure Refinement, University of Gottingen, 1993.

---

[2] Information Available: Atomic coordinates, thermal parameters, and complete bond lengths and angles for the crystal structure of 3.